MDPI

Article

Asymmetry analysis of Autler-Townes doublet in the trap-loss fluorescence spectroscopy of cesium MOT with single step Rydberg excitation

Xiaokai Hou [1], Yuewei Wang [1] , Jun He [1,2]and Junmin Wang [1,2,*]

[1] State Key Laboratory of Quantum Optics Technologies and Devices, and Institute of Opto-Electronics, Shanxi University, Tai Yuan 030006, Shanxi Province, China
[2] Collaborative Innovation Center of Extreme Optics, Shanxi University, Tai Yuan 030006, Shanxi Province, China
* Correspondence: wwjjmm@sxu.edu.cn

Abstract: Autler-Townes (AT) doublet, a fundamental manifestation of quantum interference effects, serves as a critical tool for studying the dynamic behavior of Rydberg atoms. Here, we investigate the asymmetry of the Autler-Townes (AT) doublet in trap-loss fluorescence spectroscopy (TLFS) of cesium (Cs) atoms confined in a magneto-optical trap (MOT) with single-step Rydberg excitation using a 319-nm ultraviolet (UV) laser. A V-type three-level system involving the ground state $6S_{1/2}$ (F=4), excited state $6P_{3/2}$ ($F^{'}$=5) , and Rydberg state ($nP_{3/2}$ (m_J=+3/2)) is theoretically modeled to analyze the nonlinear dependence of the AT doublet's asymmetry and interval on the cooling laser detuning. Experiments reveal that as the cooling laser detuning Δ_1 decreases from -15 MHz to -10 MHz, the AT doublet exhibits increasing symmetry, while its interval shows a nonlinear decrease. Theoretical simulations based on the density matrix equation and Lindblad master equation align closely with experimental data, confirming the model's validity. This study provides insights into quantum interference dynamics in multi-level systems and offers a systematic approach for optimizing precision measurements in cold atom spectroscopy.

Keywords: single step Rydberg excitation; trap-loss fluorescence spectroscopy

1. Introduction

Rydberg atoms [1], highly-excited atoms with principal quantum numbers n $>$ 10, have shown great promise in terms of their unique structure. These physical properties scale with principal quantum number n, such as long radiation lifetime ($\sim n^3$), strong dipole–dipole interaction ($\sim n^4$) and large polarizability ($\sim n^7$). They have found extensive applications in many-body physics [2], quantum information and computing [3,4], precision measurement [5–9]. To exploit coherent quantum dynamics, these experiments are performed on timescales shorter than the lifetime of Rydberg state. However, for the realization of supersolids [10], frustrated quantum magnetism [11] or spin squeezing for enhanced metrology [12], it is necessary to extend the investigation time of Rydberg atoms. To take advantage of the long coherence time of ground state atoms and the strong long-range interaction between Rydberg atoms, we can create a wave function that is mostly ground state with an adjustable Rydberg component by off-resonantly coupling the ground state to Rydberg state [5,13,14], which is called Rydberg dressing approach. Therefore, experimental research of Autler–Townes (AT) doublet [15] has opened a route to produce the dressed-state atoms with the long coherence time and controllable long-range

Received:
Revised:
Accepted:
Published:

Citation: Lastname, F.; Lastname, F.; Lastname, F. . *Journal Not Specified* **2025**, *1*, 0. https://doi.org/

interaction by adjusting the coupling intensity and detuning between the ground state and Rydberg state.

AT doublet, a quintessential manifestation of quantum interference effects, is characterized by key properties such as the interval, symmetry, and the width of the spectral double-peaks structure, all of which are intricately linked to parameters like the Rabi frequency and detuning of the coupling laser field [7,16,17,21]. Consequently, a comprehensive investigation of AT doublet properties is pivotal for elucidating the dynamic mechanisms Rydberg dressing ground state and for uncovering nonlinear effects in complex systems.

In this paper, we systematically investigate the characteristics of the AT doublet of the trap-loss fluorescence spectroscopy (TLFS) of in cesium (Cs) magneto-optical traps (MOT) using single-step ultraviolet (UV) laser excitation. First, a theoretical model describing the three-level V-type system of Cs atoms is established, analyzing the relationship between cooling laser detuning and AT doublet characteristics. Second, using TLFS, experimental observations of AT doublet under different cooling laser parameters are conducted, confirming that the symmetry of the AT doublet improves as detuning decreases, while the AT doublet interval exhibits a nonlinear reduction trend. Finally, a RNN architecture is employed to address the limitations of sparse experimental data by generating high-density datasets, thereby improving the precision of nonlinear fitting and parameter optimization, and further validating the applicability and stability of this approach in modeling complex physical systems.

2. The V-type three-level system with Rydberg state of Cs atoms

As depicted in Fig.1, here is a V-type three-level system comprising the Cs ground state $6S_{1/2}$ (F=4) (denoted as $|1\rangle$), the Cs atom excited state $6P_{3/2}$ ($F^{'}=5$) (denoted as $|2\rangle$), and the Cs atom Rydberg state $nP_{3/2}$ (m_J=+3/2) (denoted as $|3\rangle$). Ω_1 denotes the Rabi frequency of the excitation laser (coupling Levels $|1\rangle$ and $|2\rangle$); Δ_1 represents the detuning of the excitation laser; Γ_1 represents spontaneous decay rate of the excitation state; Ω_2 denotes the Rabi frequency of the UV laser (coupling Levels $|1\rangle$ and $|3\rangle$); and Δ_2 represents the UV laser detuning, Γ_2 represents spontaneous decay rate of the Rydberg state $|3\rangle$.

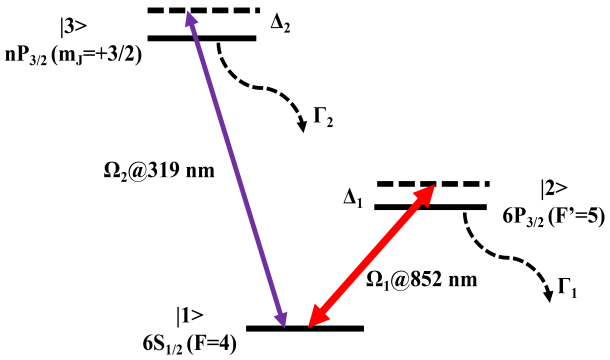

Figure 1. Schematic diagram of the V-type three level system of Cs atoms. State $|1\rangle$ ($6S_{1/2}$ (F=4)) and state $|2\rangle$ ($6P_{3/2}$ ($F^{'}$=5)) are coupled by a infrared laser (Ω_1@852 nm) with detuning Δ_1 and spontaneous decay rate Γ_1. Simultaneously, the UV laser (Ω_2@319 nm) excites Cs atoms from state $|1\rangle$ to state $|3\rangle$ ($nP_{3/2}$ (m_J=+3/2)) with corresponding detuning Δ_2 and spontaneous decay rate Γ_2. Dashed arrows indicate radiation decay channels, while solid arrows represent laser coupling pathways.

In order to explain the dynamics of the interaction between light and atoms in a V-type three-level system, we consider the following theory,

$$H = \frac{\hbar}{2}\begin{pmatrix} 0 & \Omega_1 & \Omega_2 \\ \Omega_1 & -2\Delta_1 & 0 \\ \Omega_2 & 0 & -2\Delta_2 \end{pmatrix} \tag{1}$$

$$\rho = \begin{pmatrix} \rho_{11} & \rho_{12} & \rho_{13} \\ \rho_{21} & \rho_{22} & \rho_{23} \\ \rho_{31} & \rho_{32} & \rho_{33} \end{pmatrix} \tag{2}$$

$$L(\rho) = \begin{pmatrix} \gamma_2\rho_{22} + \gamma_3\rho_{33} & -\frac{1}{2}\gamma_2\rho_{12} & -\frac{1}{2}\gamma_3\rho_{13} \\ -\frac{1}{2}\gamma_2\rho_{21} & -\gamma_2\rho_{22} & -\frac{1}{2}(\gamma_2+\gamma_3)\rho_{23} \\ -\frac{1}{2}\gamma_3\rho_{31} & -\frac{1}{2}(\gamma_2+\gamma_3)\rho_{32} & -\gamma_3\rho_{33} \end{pmatrix} \tag{3}$$

$$\dot{\rho} = -\frac{i}{\hbar}[H,\rho] + L(\rho) \tag{4}$$

Here H represents the Hamiltonian describing the interaction of the V-type three-energy-level atoms with the laser field; $\rho_{ij}(i,j=1,2,3)$ denotes the elements of the density matrix. When $i=j$, ρ_{ii} represents the diagonal elements of the density matrix, corresponding to the atomic population probabilities of each energy level. Conversely, when $i \neq j$, ρ_{ij} describes the non-diagonal elements, characterizing the coherence between two energy levels. $L(\rho)$ represents the decoherence matrix, which accounts for the dissipation processes within the system. γ_2 represents the spontaneous radiation decay rate of the cesium atom $6P_{3/2}$; while γ_3 denotes the spontaneous radiation decay rate of the cesium atom Rydberg state $nP_{3/2}$.

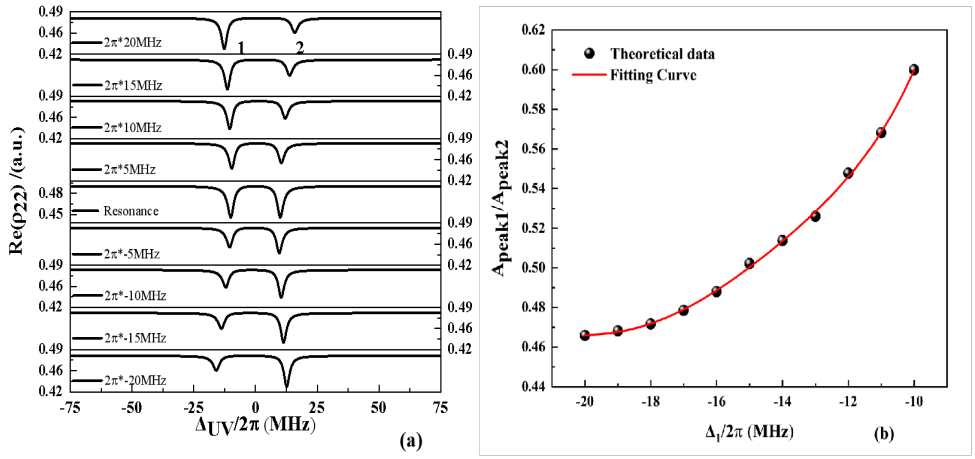

Figure 2. (a), according to Eq. (1-4), simulations are carried out to obtain the relationship between Re(ρ_{22}) and the UV laser detuning Δ_2, which exhibits an obvious AT bimodal structure; and the detuning of the excitation laser Δ_1 is constantly changed. When the detuning is gradually reduced, the AT doubleT tend to be symmetric gradually. (b), for the purpose of our actual experiments (the cooling laser frequency to maintain the normal operation of the MOT should be negatively detuned), it is taken as -20 MHz to -10 MHz, and the ratio of their respective corresponding double-peaks amplitudes. The black squares are simulated data points.The fitting curve is 5th order polynomial, the expression is $\mathbf{y = Ax^5 + Bx^4 + Cx^3 + Dx^2 + Ex + F}$, and the COD is 0.9993. Among them, the parameters A=3.13E-6, B=2.56E-4, C=8.320E-3, D=0.1341, E=1.09, F=4.149.

The TLFS [16,17,21,25] serves as a powerful tool to characterize the dynamic process of cold-atom fluorescence attenuation induced by Rydberg excitation within a MOT. In this context, cold-atom fluorescence arises from the spontaneous radiation of the excited state,

rendering it directly proportional to the atomic population probability of the excited state. Utilizing Eq. (1–4), we derive the instantaneous steady-state solution, incorporating the temporal density matrix, to analyze the population probability ρ_{22} of energy level 2.

As depicted in Fig. 2, the excitation laser Rabi frequency Ω_1, and the UV laser Rabi frequency Ω_2 are held constant, while the UV laser detuning, and scan the UV laser detuning Δ_2 is scanned to generate the double-peak spectral structure. Since the vertical axis represents the atomic population probability of excited state 2, which is directly proportional to the fluorescence intensity of the cold atoms, this simulation effectively characterizes the physical behavior of cold atoms in a MOT with reduced fluorescence due to Rydberg excitation. In this spectrum, Peaks 1 and 2 correspond to the double peaks of the AT doublet. These peaks exhibit increased symmetry as the excitation laser detuning approaches resonance, while the interval between the peaks expands with increasing excitation laser detuning. We fit the data using a 5th-order polynomial with an expression $\mathbf{y = Ax^5 + Bx^4 + Cx^3 + Dx^2 + Ex + F}$ and the coefficient of determination (COD) of 0.9993. Among them, the parameters A=3.13E-6, B=2.56E-4, C=8.320E-3, D=0.1341, E=1.09, F=4.149.

3. Trap-loss fluorescence spectroscopy and AT doublet in Cs MOT

As illustrated in Fig. 3, the image on the left shows the atomic energy level diagram of the MOT and the single-step Rydberg excitation. The thick red arrow represents the cooling laser beam, and its Rabi frequency is marked Ω_1, and the detuning is Δ_1; The thin red arrow represents the repumping laser beam, which is used to pump the atoms populated on $6S_{1/2}$ (F=3) to continue to participate in the cooling process; The purple arrow represents the UV laser beam for single-step Rydberg excitation, with a Rabi frequency labeled Ω_2 and a detuned as Δ_2. The above marks correspond one-to-one to Fig. 1 in the theoretical part, however, where we ignore the behavior that the atoms will populate in $6S_{1/2}$ (F=3), i.e., the repumping laser is not considered. And, in the Fig.3 (b), the Cs MOT is housed within a $30 \times 30 \times 120$ mm^3 ultra-high vacuum (UHV) glass cell, with typical pressure of approximately 1×10^{-9} Torr. The frequency of the cooling laser beam, which has a Gaussian diameter of approximately 10 mm, is locked to the Cs $6S_{1/2}$ (F=4) $\rightarrow$ $6P_{3/2}$ ($F^{'}$=5) cycling transition with a detuning Δ_1. The repumping laser beam, with a Gaussian diameter of around 9 mm, is resonant with the Cs $6S_{1/2}$ (F=3) $\rightarrow$ $6P_{3/2}$ ($F^{'}$=4) transition. The cooling laser beam and repumping laser beams are combined and then are divided into three parts: one part along the Z and -Z directions, accounting for approximately 40% of the power. The remaining two parts are split equally in power and directed in the XY plane at an angle of about 80°. A gradient magnetic field is produced by a pair of anti-Helmholtz coils driven by a constant-current source, generating a typical axial magnetic field gradient of 10 Gauss/cm with a current of 9 A. Consequently, a bright cloud of cold atomic ensemble can be immediately observed using a CCD camera.

Since a MOT cannot trap Rydberg atoms, Rydberg atoms are lost when the UV laser[26–29] couples Cs atoms from the $6S_{1/2}$ (F=4) to the $nP_{3/2}$ (m_J=+3/2) state, achieving single-step Rydberg excitation. In other words, the excitation of Rydberg atoms can be inferred by observing the trap-loss fluorescence from a cold cloud in the MOT.

During the experiment, the change in frequency of our UV laser system is achieved by scanning it point by point. Each frequency point lasts for 30 s. The CCD camera is triggered for taking the photograph of the cold atom within 30 s, the timestamp of the initial trigger is synchronized, which occurs 5 s after the UV laser is adjusted to the target frequency, and taking the photograph ends at the next time the UV laser frequency is modified, the exposure time of the CCD camera is 5 ms, and the CCD's trigger frequency is 0.2 Hz. In a spectrum acquisition process, each frequency point lasts for 30 s, and the

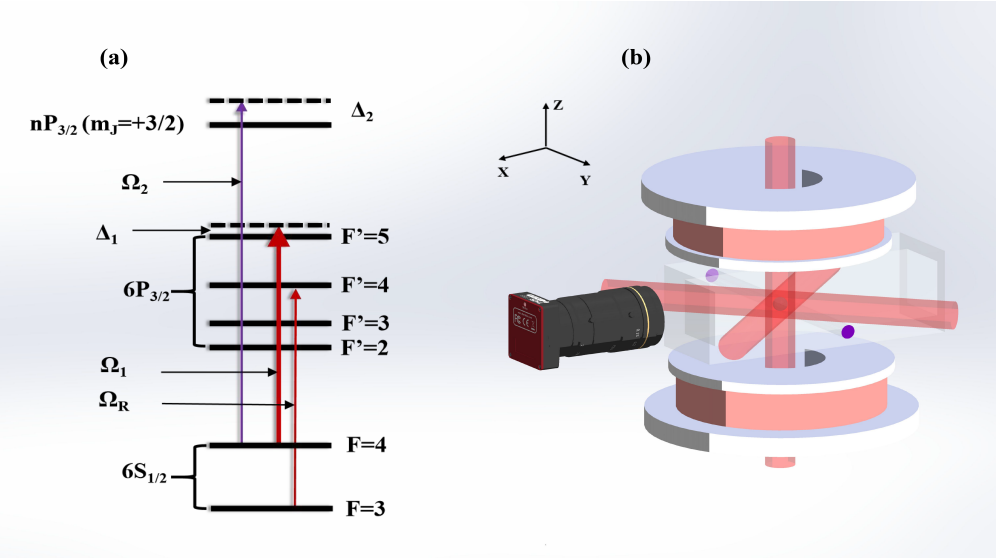

Figure 3. Diagram of Cs relevant energy level and MOT setup. (a) displays the atomic energy level diagram, emphasizing the cooling laser beam (thick red arrows) and repumping laser beam (thin red arrows) and UV laser beam (purple arrows) for single-step Rydberg excitation. (b) presents the experimental configuration, featuring the trapping region surrounded by a pair of coils generating a quadrupole magnetic field and the intersection of laser beams for cooling. The imaging system, aligned along a principal axis, enables precise monitoring of atomic fluorescence.

UV laser frequency needs to be changed about 45∼55 times, covering about 175∼200 MHz, with a total duration of about 30 minutes.

Since the UV Rabi frequency is the order of several hundred kHz, the Rydberg excitation time is must less than the CCD exposure time. Therefore, we believe that the loss of atomic number in the MOT is completely at a steady state within the 5 ms time window. Within 30 s, five fluorescence images of cold atoms will be obtained, and three of them will be randomly selected to calibrate the remaining proportion of cold atoms in the MOT at the current UV laser frequency. For every five data acquisitions, we will take pictures of the MOT that are not Rydberg excited by UV laser for image processing and fluorescence intensity normalization for these five data acquisitions. After a spectral data acquisition, we use a MATLAB program to process the fluorescence images of cold atoms, and the relative fluorescence intensity is calculated by dividing the total fluorescence intensity of the cold atoms in the MOT with UV laser excitation by the reference fluorescence intensity without UV laser excitation. In addition, background light was subtracted to correct for the effect of background scattered light.

Throughout the experiment, we utilize a wavelength meter (HighFinesse, WS-7) to monitor the red light frequency in real time, ensuring the accuracy of the UV frequency. Additionally, the wave meter is calibrated after every five acquisitions using the probe beam ($6S_{1/2}$ (F=4) $\rightarrow$ $6P_{3/2}$ ($F^{'}$=5), 351.72196 THz [30]) as the frequency reference.

We select $71P_{3/2}$ as the target Rydberg state, experimentally observe the TLFS and its AT doublet, and investigat the dependence of AT doublet characteristics on laser detuning. Specific results are given in [7,17] In this paper, we only analyze the symmetry and interval of the AT doublet of the TLFS. As shown in Fig. 4, we fixed the Rabi frequency Ω_1 of the cooling laser beam to $2\pi \times 8.1$ MHz and the UV laser Rabi frequency Ω_2 to $2\pi \times 117$ kHz, and gradually decreased the cooling laser detuning Δ_1 (-15, -14, -13, -12, -11, -10 MHz). Here, we present only three of these sets of data ((top): -10 MHz; (middle): -12 MHz; (bottom): -15 MHz), and the specific results can be found in Ref [17]. The ratio of the amplitudes of the AT doublet (peaks 1 and 2) gradually decreases with the increase

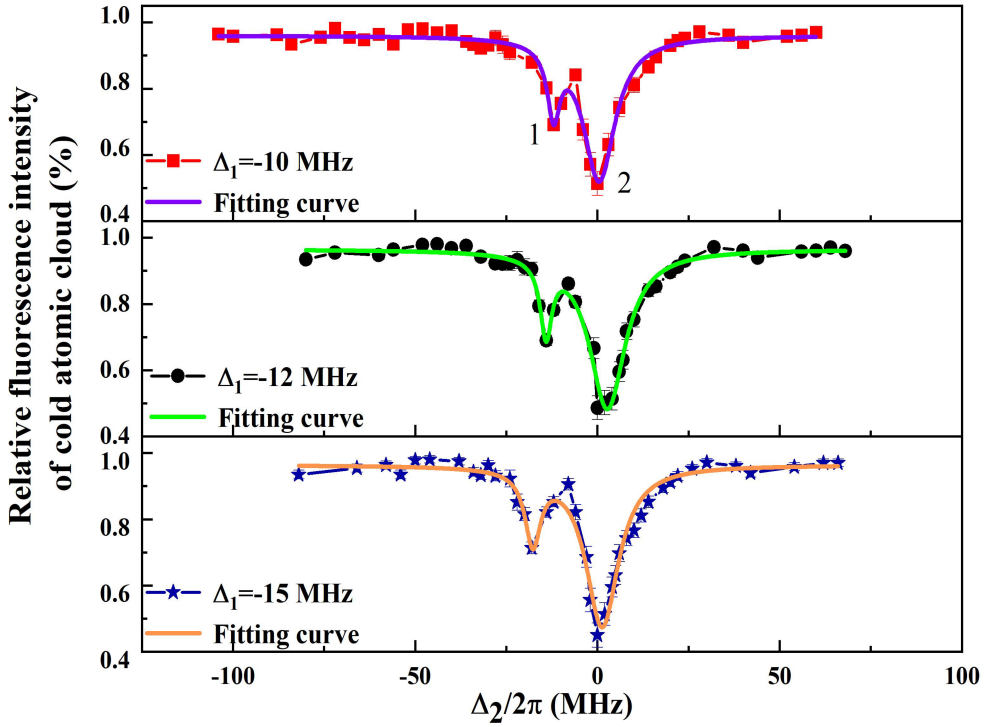

Figure 4. The TLFS and their AT doublet at different amounts of cooling laser detuning. By adjusting the parameters, a significant change in the resonance signal can be observed. Among them, the cooling laser Rabi frequency is fixed to $2\pi \times 8.1$ MHz, and the Rabi frequency of UV laser is $2\pi \times 117$ kHz, and the detuning of cooling laser is gradually reduced, and three sets of spectral signals ((top): -10 MHz; (Medium): -12 MHz; (bottom): -15 MHz). The amplitude ratio of peaks 1 and 2 gradually increases, tends to be asymmetrical, and the AT doublet interval also increases gradually with the increase of cooling laser detuning. The red squares, black circles, and blue stars are experimental data, and the purple, green, and orange curves are multi-peaks Lorentzian profile fitting curves.

of the cooling laser detuning, i.e., the double-peaks gradually tend to be asymmetric; and according to $\tilde{\Omega} = \sqrt{\Omega_1^2 + \Delta_1^2}$, the intervals of the AT doublet gradually decrease with the decrease of the detuning.

However, to our surprise, the full width at half maximum (FWHM) of the TLFS measured at four different principal quantum numbers was all on the order of 20 MHz. We propose five possible mechanisms for the linewidth broadening of the TLFS:

Firstly, the Rabi frequency of the cooling laser is still at a relatively high order of magnitude, which still causes the ground state is broadened by a factor of 1.7 due to power broadening. Secondly, The Zeeman broadening in the z-direction at the center of the MOT can be calculated according to $\Delta\Gamma = \frac{\mu_B}{h} g_J(S_{1/2}) \frac{\partial B}{\partial z} \Delta z$. The ground state $6S_{1/2}$ broadens to 0.96 MHz due to the presence of a magnetic field. Thirdly, our atoms are exposed to severe blackbody radiation (BBR) at room temperature that will directly couple the target Rydberg state with the adjacent Rydberg state. So, the lifetime of the target Rydberg state decreases dramatically, and the typical Rydberg state lifetime is about 10 μs, and the width of the Rydberg state energy level is broadened to 100 kHz. Fourth, as can be seen in Fig. 4, the baseline is less than 100% at the UV laser separation resonance position, there is still a 15% $\sim$ 20% loss of cold atomic fluorescence intensity. This is due to the fact that the cold atoms in the magneto-optical trap are constantly affected by ionization, and we speculate that the mechanisms that lead to ionization are photoionization, field ionization, and collision ionization. Due to the presence of ionization, the overall spectral signal increases by 15% $\sim$ 20%, then we can simply infer that the spectral linewidth is broadened

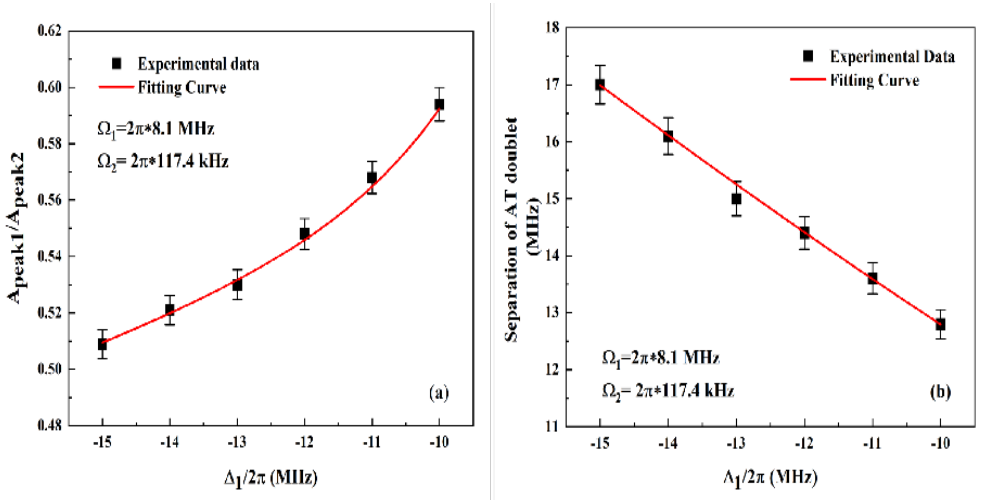

Figure 5. Comparative analysis of experimental results obtained under varying laser detuning (−15, −14, −13, −12, −11, −10 MHz). (a) The black data points illustrate the trend of the AT doublet amplitude ratio as a function of the cooling laser detuning, with uncertainties indicated by error bars. (b) The black data points represent the AT doublet interval, while the nonlinear dependence predicted by the theoretical model is highlighted through the red solid line fitting.

by at least 15% due to the presence of ionization. Last, due to the existence of the ionization mechanism, a cold plasma is formed near the cold atoms, which in turn generates a local electric field of a certain intensity, whose electric field intensity is space-dependent. When such a local electric field is superimposed with the background DC electric field, the Stark shift formed on the Rydberg state will be spatially dependent. It can be roughly inferred that the remaining broadening of about 5 MHz comes from the local electric field generated by the cold plasma [31].

Figure 5(a) illustrates the relationship between AT doublet symmetry and cooling laser detuning experimentally, and we select the range of laser detuning of $-15\sim-10$ MHz with the step of 1 MHz. It can be seen that the variation trend of the black data points is consistent with that of Fig. 2(b), and the AT doublet gradually tend to be symmetrical as the amount of cooling laser detuning decreases. The red curve is the fitting function, which is still a 5-order polynomial, and the parameters remain unchanged, with a COD of 0.9451. This shows that the theoretical model is in good agreement with the experimental data. Fig. 5(b) shows the AT doublet splitting interval with cooling laser detuning in the three sets of spectra. With the decrease of the cooling laser detuning, the double-peak interval tends to decrease, and we use the formula with the expression $\tilde{\Omega} = A\sqrt{\Omega_1^2 + \Delta_1^2}$, where A is the correction parameter, the specific value is 0.91, and the COD is 0.9997.

4. Conclusions

In this paper, we systematically analyze the behavior of AT doublet asymmetry in the MOT of Cs atom through theoretical modeling and experiments. We used a 319 nm UV laser to excite the ground state atoms $6S_{1/2}$ (F=4) to the Rydberg state $71P_{3/2}$ (m_J=3/2) by a single step Rydberg excitation, and obtained the TLFS by all-optical non-destructive detection. Due to the presence of strong cooling laser, we also clearly observed the AT doublet of the TLFS, and comprehensively analyzed the relationship between the asymmetry of the AT doublet and the detuning of the cooling laser by establishing a V-typed three-level system model. The results are pivotal for elucidating the dynamic mechanisms Rydberg dressing ground state and for uncovering nonlinear effects in complex systems and have positive significance for further development of quantum information processing and quantum computing in the cold atoms.

Author Contributions: For research articles with several authors, a short paragraph specifying their individual contributions must be provided. The following statements should be used "Conceptualization, J. M. Wang and X. K. Hou; methodology, X. K. Hou; software, X. K. Hou; validation, X. K. Hou, and Y. W. Wang; formal analysis, X. K. Hou; investigation, X. K. Hou; writing—original draft preparation, X. K. Hou; writing—review and editing, X. K. Hou, J. M. Wang, and J. He; visualization, X.X.; supervision, J. M. Wang; project administration, J. M. Wang; funding acquisition, J. M. Wang. All authors have read and agreed to the published version of the manuscript.", please turn to the CRediT taxonomy for the term explanation. Authorship must be limited to those who have contributed substantially to the work reported.

Funding: This research was funded by the National Key R & D Program of China (2021YFA1402002), the National Natural Science Foundation of China (12474483), and the Fundamental Research Program of Shanxi Province (202403021211013

Data Availability Statement: We encourage all authors of articles published in MDPI journals to share their research data. In this section, please provide details regarding where data supporting reported results can be found, including links to publicly archived datasets analyzed or generated during the study. Where no new data were created, or where data is unavailable due to privacy or ethical restrictions, a statement is still required. Suggested Data Availability Statements are available in section "MDPI Research Data Policies" at https://www.mdpi.com/ethics.

Acknowledgments: In this section you can acknowledge any support given which is not covered by the author contribution or funding sections. This may include administrative and technical support, or donations in kind (e.g., materials used for experiments).

Conflicts of Interest: Declare conflicts of interest or state "The authors declare no conflicts of interest." Authors must identify and declare any personal circumstances or interest that may be perceived as inappropriately influencing the representation or interpretation of reported research results. Any role of the funders in the design of the study; in the collection, analyses or interpretation of data; in the writing of the manuscript; or in the decision to publish the results must be declared in this section. If there is no role, please state "The funders had no role in the design of the study; in the collection, analyses, or interpretation of data; in the writing of the manuscript; or in the decision to publish the results".

References

1. T. F. Gallagher, "Rydberg atoms," Cambridge University Press, 2005.
2. A. Browaeys and T. Lahaye, "Many-body physics with individually controlled Rydberg atoms," *Nature Physics*, vol. 16, no. 2, p. 132–142, 2020.
3. C. S. Adams, J. D. Pritchard, and J. P. Shaffer, "Rydberg atom quantum technologies," *Journal of Physics B: Atomic, Molecular and Optical Physics*, vol. 53, no. 1, 012002, 2019.
4. M. Saffman, T. G. Walker, and K. Mølmer, "Quantum information with Rydberg atoms," *Reviews of Modern Physics*, vol. 82, no. 3, 2313, 2010.
5. A. Arias, G. Lochead, T. M. Wintermantel, S. Helmrich, and S. Whitlock, "Realization of a Rydberg-dressed Ramsey interferometer and electrometer," *Physical Review Letters*, vol. 122, no. 5, 053601, 2019.
6. M. Y. Jing, Y. Hu, J. Ma, H. Zhang, L. J. Zhang, L. T. Xiao, and S. T. Jia, "Atomic superheterodyne receiver based on microwave-dressed Rydberg spectroscopy," *Nature Physics*, vol. 16, no. 9, p. 911–915, 2020.
7. J. D. Bai, S. Liu, J. Y. Wang, J. He, and J. M. Wang, "Single-photon Rydberg excitation and trap-loss spectroscopy of cold cesium atoms in a magneto-optical trap by using of a 319-nm ultraviolet laser system," *IEEE Journal of Selected Topics in Quantum Electronics*, vol. 26, 1600106, 2020.
8. D. A. Anderson, S. A. Miller, G. Raithel, J. A. Gordon, M. L. Butler, and C. L. Holloway, "Optical measurements of strong microwave fields with Rydberg atoms in a vapor cell," *Physical Review Applied*, vol. 5, no. 3, 034003, 2016.
9. S. Kumar, H. q. Fan, H. Kübler, A. J. Jahangiri, and J. P. Shaffer, "Rydberg-atom based radio-frequency electrometry using frequency modulation spectroscopy in room temperature vapor cells," *Optics Express*, vol. 25, no. 8, p. 8625–8637, 2017.
10. M. Boninsegni, H. q. Prokof'ev, "Colloquium: supersolids: what and where are they?," *Reviews of Modern Physics*, vol. 84, 759, 2012.

11. A. W Glaetzle, M. Dalmonte, R. Nath, C. Gross, I. Bloch, P. Zoller, "Designing frustrated quantum magnets with laser dressed Rydberg atoms," *Physical Review Letters*, vol. 114, 173002, 2015.
12. L. I. R. Gil, R. Mukherjee, E. M. Bridge, M. P. A. Jones, T. Pohl, "Spin squeezing in a Rydberg lattice clock," *Physical Review Letters*, vol. 112, 103601, 2014.
13. J. Lee, M. J. Martin, Y. Y. Jau, T. Keating, T.H. Deutsch, G. W. Biedermann, "Demonstration of the Jaynes–Cummings ladder with Rydberg-dressed atoms," *Physical Review A*, vol. 95, 041801(R), 2017.
14. Y. Y. Jau, A. M. Hankin, T. Keating, T.H. Deutsch, G. W. Biedermann, "Entangling atomic spins with a Rydberg-dressed spin-flip blockade," *Nature Physics*, vol. 12, p. 71–74, 2016.
15. S. h. Aulter, C. h. Townes, "Stark effect in rapidly varying fields," *Physical Review*, vol. 100, no. 2, p. 703–723, 1955.
16. J. D. Bai, J. Y. Wang, S. Liu, J. He, and J. M. Wang, "Autler–Townes doublet in single-photon Rydberg spectra of cesium atomic vapor with a 319 nm UV laser," *Applied Physics B*, vol. 125, no. 3, 33, 2019.
17. X. Wang, X. K. Hou, F. F. Lu, R. Chang, L. L. Hao, W. J. Su, J. D. Bai, J. He, and J. M. Wang, "Autler–townes doublet in the trap-loss fluorescence spectroscopy due to single-step direct Rydberg excitation of cesium cold atomic ensemble," *AIP Advances*, vol. 13, no. 3, 035126, 2023.
18. D. A. Braje, V. Balić, S. Goda, G. Y. Yin, S. E. Harris, "Frequency mixing using electromagnetically induced transparency in cold atoms," *Physical Review Letter*, vol. 93, 183601, 2004.
19. L. V. Hau, S. E. Harris, Z. Dutton, C. H. Behroozi, "Light speed reduction to 17 meters per second in an ultracold atomic gas," *Nature*, vol. 397, p. 594-598, 1999.
20. U. Raitzsch, R. Heidemann, H. Weimer, B. Butscher, P. Kollmann, R. Löw, H. P. Büchler, T. Pfau, "Investigation of dephasing rates in an interacting Rydberg gas," *New Journal of Physics*, vol. 11, 055014, 2009.
21. Y. F. Cao, W. G. Yang, H. Zhang, M. Y. Jing, W. B. Li, L. J. Zhang, L. T. Xiao, and S. T. Jia, "Dephasing effect of Rydberg states on trap loss spectroscopy of cold atoms," *Journal of the Optical Society of America B*, vol. 39, no. 8, p. 2032–2036, 2022.
22. E. H. Ahmed, S. Ingram, T. Kirova, O. Salihoglu, J. Huennekens, J. Qi, Y. Guan, A. M. Lyyra, "Quantum control of the spin-orbit interaction using the Autler-Townes effect," *Physical Review Letters*, vol. 107, 163601, 2011.
23. L. Phuttitarn, M. Becker, R. Chinnarasu, M. Graham, M. Saffman, "Enhanced measurement of neutral-atom qubits with machine learning," *Physical Review Applied*, vol. 22, 024011, 2024.
24. X. Meng, Y. W. Zhang, X. C. Zhang, S. C. Jin, T. R. Wang, L. Jiang, L. T. Xiao, S. T. Jia, Y. H. Xiao, "Machine learning assisted vector atomic magnetometry," *Nature Communications*, vol. 14, 6105, 2023.
25. C. Halter, A. Miethke, C. Sillus, A. Hegde, and A. Göerlitz, "Trap-loss spectroscopy of Rydberg states in ytterbium," *Journal of Physics B : Atomic, Molecular and Optical Physics*, vol. 56, 055001, 2023.
26. J. Y. Wang, J. D. Bai, J. He, and J. M. Wang, "Realization and characterization of single-frequency tunable 637.2 nm high-power laser," *Optics Communications*, vol. 370, p. 150–155, 2016.
27. J. Y. Wang, J. D. Bai, J. He, and J. M. Wang, "Development and characterization of a 2.2 W narrow-linewidth 318.6 nm ultraviolet laser," *Journal of the Optical Society of America B*, vol. 33, no. 10, p. 2020–2025, 2016.
28. J. D. Bai, J. Y. Wang, J. He, and J. M. Wang, "Electronic sideband locking of a broadly tunable 318.6 nm ultraviolet laser to an ultra-stable optical cavity," *Journal of Optics*, vol. 19, 045501, 2017.
29. J. M. Wang, J. D. Bai, J. Y. Wang, S. Liu, B. D. Yang, and J. He, "Realization of a watt-level 319-nm single-frequency cw ultraviolet laser and its application in single-photon Rydberg excitation of cesium atoms [invited]," *Chinese Optics*, vol. 12, no. 4, p. 701–718, 2019 (in Chinese).
30. A. Kramida, Yu. Ralchenko, J. Reader, (NIST ASD Team) (2024), "NIST Atomic Spectra Database (version 5.12)," Available: https://physics.nist.gov/asd [Nov 12 2024].
31. M. P. Robinson, B. L. Tolra, M. W. Noel, T. F. Gallagher, and P. Pillet, "Spontaneous evolution of Rydberg atoms into an ultracold plasma," *Physical Review Letters*, vol. 85, no. 21, p. 4466–4469, 2000.